Journal of Inclusion Phenomena and Macrocyclic Chemistry (2006) 56: 261–273
DOI 10.1007/s10847-006-9093-2

Interaction of Valdecoxib with β-cyclodextrin: Experimental and Molecular Modeling Studies

GANESH S. JADHAV[1], ASHOK R. PATEL[1], PRADEEP R. VAVIA[1,*], ALPESHKUMAR K. MALDE[2] and EVANS C. COUTINHO[2]
[1]*Pharmaceutical Division, Mumbai University Institute of Chemical Technology, 400 019, Matunga, Mumbai, India;*
[2]*Department of Pharmaceutical Chemistry, Bombay College of Pharmacy, 400 098, Kalina, Mumbai, India*

Key words: β-cyclodextrin, complexation, dissolution studies, molecular modeling, solubility, valdecoxib

Abstract

This study aimed to investigate the effect of β-cyclodextrin on aqueous solubility and dissolution rate of valdecoxib and also to get an insight of molecular interactions involved in formation of valdecoxib-β-cyclodextrin inclusion complex. Phase solubility analysis indicated complex with possible stoichiometry of 1:1 and a stability constant of 234.01 M^{-1}. Thermodynamic studies in water indicated exothermic nature of inclusion complexation. Valdecoxib-β-cyclodextrin complexes (1:1 M) were prepared by kneading method, solution method and freeze–drying method. The complex was characterized by differential scanning calorimetry (DSC), powder X-ray diffractometry (P-XRD), Fourier transform infrared (FTIR) spectroscopy and nuclear magnetic resonance (^{1}H-NMR) spectroscopy. Molecular modeling was used to help establish the mode of interaction of β-cyclodextrin with valdecoxib. ^{1}H-NMR analysis suggested that the unsubstituted phenyl ring of valdecoxib display favorable interaction with the hydrophobic cavity of β-cyclodextrin, which was confirmed by molecular dynamic simulations. An inclusion complex model has been established for explaining the observed enhancement of solubility of valdecoxib in water by β-cyclodextrin. Dissolution studies in water showed that the valdecoxib in freeze-dried complex dissolved much faster than the uncomplexed drug and physical mixture. This improvement in dissolution rate is attributed to the increased solubility and wettability due to encapsulation along with decreased crystallanity caused by complex formation, which is evident by DSC and P-XRD studies.

Abbreviations: DSC – differential scanning calorimetry; P-XRD – powder X-ray diffractometry; FTIR – Fourier transform infrared; ^{1}H-NMR – proton-nuclear magnetic resonance; CDs – cyclodextrins; VAL – Valdecoxib; BCD – β-cyclodextrin; KM – kneading method; SM – solution method; FD – freeze–drying method; PM – physical mixture; DMSO – dimethylsulfoxide; TMS – tetramethylsilane; RDC – relative degree of crystallanity; MD – molecular dynamics; TPSA – total polar surface area; THSA – total hydrophobic surface area; DE – dissolution efficiency; DP – percentage of dissolved drug; RDR – relative drug release (with reference to pure drug)

Introduction

Majority of the compounds being developed by the pharmaceutical industry are poorly water soluble lipophilic compounds (Biopharmaceutical Classification System, BCS class II or class IV). A limiting factor to the *in-vivo* performance of such drugs after oral administration is their inadequate ability to be wetted by and dissolved into the gastrointestinal fluid. Therefore, increasing the dissolution rate of such drugs is an important and significant challenge to formulation scientists. Several approaches (salt formation, prodrug, micronization, solid dispersions, solvates, adsorbates, or complexes) are employed to overcome the limiting aqueous solubility [1]. Cyclodextrins (CDs) have attracted growing interest in the pharmaceutical industry as complexing agents because of their low toxicity and ability to produce stable inclusion complexes [2, 3]. They are torous-shaped oligosaccharides produced by enzymatic hydrolysis and cyclization of starch, containing six (α-CD), seven (β-CD), or eight (γ-CD) α-1, 4-linked D-glucopyranose units, containing relatively hydrophobic central cavity and hydrophilic outer surface. CDs are not perfectly cylindrical molecules but are toroidal or cone shaped due to lack of free rotation about the bonds connecting the glucopyranose units (Figure 1). Thus, the primary hydroxyl groups are located on the narrow side, while the secondary hydroxyl

* Author for correspondence. E-mail: vaviapradeep@yahoo.com

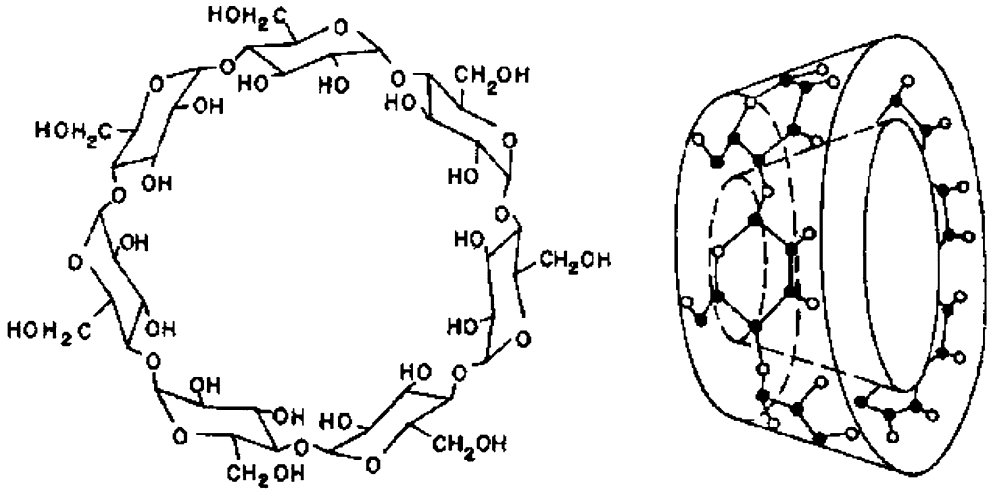

Figure 1. Chemical Structure of β-cyclodextrin (toroidal shape).

groups are located on the wider edge. CDs have been used extensively to increase the aqueous solubility, stability and bioavailability of drugs [4]. The solubilizing abilities of CDs have been attributed to the formation of inclusion complexes between CDs and the 'guest' drug molecules. Generally, this complexation involves the inclusion of 'guest' molecule in the cavity of a 'host' molecule, such as CDs, with no covalent bonding [5].

Valdecoxib (VAL) (Figure 2) is a novel and specific cycloxygenase-2 (COX-2) inhibitor exhibiting anti-inflammatory, analgesic and antipyretic properties with a lower incidence of ulcer complications [6–8]. However, valdecoxib is practically insoluble in water (0.01 mg/ml) and classified as BCS class II drug having low solubility and high permeability [9]. The very poor aqueous solubility and wettability of the drug leads to erratic absorption, delayed onset of action ($T_{max} = 2.25$ h) and variable bioavailability [10]. To overcome these drawbacks, enhancement of aqueous solubility of VAL is necessary. β-cyclodextrin (BCD) was chosen, although it has limited aqueous solubility, to enhance the solubility of valdecoxib due to its central cavity diameter (6–6.5 Å) appropriate to accommodate most of aromatic rings, efficiency of drug complexation, availability in pure form, and relatively low cost. Absorption of BCD in an intact form is limited because of their bulky and hydrophobic nature. Hence, BCDs act as true carriers by keeping the hydrophobic drug molecules in solution and delivering them to the surface of the biological membrane such as gastrointestinal mucosa, where they partition into the membrane [11].

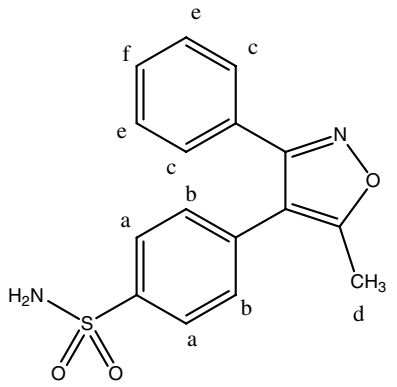

Figure 2. Chemical Structure of Valdecoxib (VAL).

The synergistic play between exhaustive molecular modeling studies and experiment can help to understand the nature of the inclusion complexes, particularly their structure, energies, and stoichiometries [12]. The use of molecular mechanics [13] and dynamic simulations [14] has previously been reported in the study of cyclodextrin complexes. Docking programs have also been used to study inclusion complexes for qualitative purposes [15].

The present work attempted to investigate the feasibility of utilizing BCD to improve aqueous solubility and dissolution rate of VAL and also to elucidate the mode of complexation between VAL and BCD. With these objectives in mind, phase solubility studies at various temperatures were carried out to find out thermodynamic parameters of inclusion phenomenon. DSC, P-XRD, FTIR and ^{1}H-NMR have been employed together with molecular modeling as a complementary tool for characterizing the complex of VAL-BCD.

Experimental

Materials

VAL was used as supplied by Unichem Lab. Ltd. Mumbai, India. BCD was generously donated by Cerestar Inc., USA. All other materials and solvents were of analytical reagent grade. Double-distilled water was used throughout the study.

Methods

Phase solubility studies

Solubility studies were carried out according to the method reported by Higuchi and Connors [16]. Excess

amounts of VAL were added to aqueous solutions (pH 6.2 ± 0.1) containing increasing concentrations of BCD (2.0×10^{-3} M to 14×10^{-3} M) and the samples were shaken at 25, 40, 50 and 60 ± 0.3 °C, until solubility equilibria were reached. After equilibration, aliquots of the supernatant were filtered through a membrane filter (0.22 μm, Sartorious cellulose nitrate filter, Germany). The filtrates were then suitably diluted with water and analyzed using UV spectrophotometer (Shimadzu 160A UV/Vis spectrophotometer, Shimadzu Corp., Kyoto, Japan) at 239 nm.

Preparation of solid complexes

VAL–BCD complexes of 1:1 M ratios were prepared by following methods.

kneading method (KM): Physical mixture of VAL and BCD in 1:1 M was triturated in a mortar with a small volume of water-methanol (1:1 v/v) solution. The thick slurry was kneaded for approximately 45 min and then dried at 45 °C. The dried mass was pulverized and passed through 100-mesh sieve.

Solution method (SM): The aqueous solution of BCD was added to alcoholic solution of VAL in 1:1 M ratio. The resulting mixture was stirred for 24 h and evaporated under vacuum at a temperature of 45 °C. The solid residue was further dried completely at 40 °C for 48 h. The dried mass was pulverized and passed through 100-mesh sieve.

Freeze–Drying Method (FD): The required 1:1 M stoichiometric quantity of VAL was dispersed in an aqueous solution of BCD while mixing with a magnetic stirrer at room temperature. After agitation for 7 days at room temperature, the suspension was filtered through membrane filter (0.22 μm, Sartorious cellulose nitrate filter, Germany). The filtrate was frozen at −70 °C and then lyophilized using LABCONCO, Freeze Dry System, Freezone 4.5.

Physical mixture (PM): A physical mixture of VAL and BCD in 1:1 M ratio was prepared by mixing the individual components (that had previously been passed through 100-mesh sieve) together in geometric proportions.

Characterization of complexes

Differential Scanning Calorimetry (DSC): Thermograms of pure materials (VAL, BCD), PM and FD complex were recorded on a Perkin–Elmer DSC 7 model. About 10 mg samples were sealed in aluminium pans and heated at a rate of 10 °C/min from 30–210 °C.

Powder X-ray Diffractometry (P-XRD): The powder X-ray diffraction patterns of pure materials (VAL, BCD), PM and FD complex were recorded on a Philips X-ray diffractometer (PW 1710, Philips Analytical, Almelo, The Netherlands) with a copper target, voltage 40 kV, current 30 mA, and a scanning rate of 1°/min.

Fourier transform infrared (FTIR) Spectroscopy: Fourier transform infrared (FTIR) spectra of pure materials (VAL, BCD), PM and FD complex were obtained in the range of 400–4600 cm^{-1} using a Jasco-FTIR spectrophotometer (Jasco, Essex, UK) by KBr disc method.

Nuclear magnetic resonance (NMR) Spectroscopy: ^{1}H-NMR spectroscopic analysis were performed on Bruker AMX-500 Fourier transform nuclear magnetic resonance (FT-NMR) spectrophotometer (Bruker AXS Inc, Madison, WI) at 298 K with an operating frequency of 500 MHz. The 5-mM samples (VAL, BCD) and equivalent to 5-mM of individual components (VAL–BCD complex) were prepared in dimethylsulfoxide-d_6 (DMSO-d_6). Chemical shifts were reported in ppm (δ) downfield from tetramethylsilane, TMS (internal reference).

Molecular modeling studies

Molecular mechanics and dynamics calculations were carried out on a Pentium 2.8 GHz PC with Linux OS (Red Hat Enterprise WS 3.0) using the *Discover* (Accelrys, Inc., USA) molecular modeling software. The initial coordinates for BCD were obtained from the Protein Data Bank with the accession code 1BFN [17]. The partial charges and potentials were calculated using the Consistent Valence force field (CVFF). A single drug molecule was docked manually into the cavity formed by secondary hydroxyls (2′-OH) on one side of BCD. The resulting complex was minimized using steepest descents followed by conjugate gradients to a gradient convergence of 0.001 kcal/mol/Å. The complex was then subjected to a 5 ps molecular dynamics (MD) simulation at 298 K with a step size of 1 fs. The trajectory was analyzed to locate the minimum energy complex and it was further minimized as above said protocol. The resulting complex was analyzed for inter-molecular interactions, interaction energies and mode of drug binding. Jurs descriptors, namely total polar surface area (TPSA) and total hydrophobic surface area (THSA) were calculated for VAL, BCD and VAL-BCD complex.

In vitro *dissolution studies*

The dissolution studies were performed in a USP dissolution apparatus number II (rotating paddle type). Accurately weighed complexes equivalent to 20 mg of VAL were spread over 900 ml of dissolution medium (distilled water, pH 6.2 ± 0.1). The stirring speed employed was 75 rpm, and the temperature was maintained at 37 ± 0.5 °C. Ten milliliter aliquots of dissolution media were withdrawn at predetermined time intervals and replaced by 10 ml of fresh dissolution media. The filtrates of samples were analyzed for VAL content by UV spectrophotometer at 239 nm. The experiments were done in triplicate. The dissolution profiles were evaluated on the basis of dissolution efficiency (DE) parameters at 20 and 60 min and dissolved percentage (DP) at 20 and 60 min. Dissolution efficiency was calculated from the area under the curve of dissolution versus time (measured using the trapezoidal rule) and expressed as a percentage of the area of the

rectangle described by 100% dissolution in the same time [18]. Relative dissolution rate (RDR) was calculated as ratio between amount of the drug dissolved from sample and that dissolved from pure drug alone at the same time interval. One-way analysis of variance (ANOVA) was used to test the significance of the differences between pure and other samples. Significance of differences in the means were tested at 95% confidence level.

Results

Phase solubility studies

Phase solubility analysis is an important tool to study inclusion complexation phenomenon of drugs with CDs in water because it gives information about the solubilizing ability of the host molecules, moreover, stability constant of complexes can be calculated by analysis of solubility curve [19]. The phase solubility profile for the complex formation between VAL and BCD at 25 °C is shown in the Figure 3. There is linear increase in the solubility of VAL with increasing concentrations of BCD and exhibiting A_L-type of solubility curve showing that soluble complexes were formed and no precipitation was observed [16] over the entire concentration range studied. This linear host-guest correlation with a slope less than 1 suggested the formation of first order soluble complexes. The apparent 1:1 stability constant, K_C was calculated from the straight line of the phase solubility diagram by using following equation,

$$K_C = \frac{\text{Slope}}{\text{Intercept} \times (1 - \text{Slope})}$$

The K_C value is a useful index to estimate the degree of binding strength of the complex. The K_C value of the inclusion complexation can be altered by changing the reaction conditions like dilution, temperature, pH and addition of excipients [20]. The K_C value for the VAL–BCD complex was found to be 234.01 M^{-1}.

The aqueous solubility of VAL, in presence of BCD, increased with elevation of temperature (25, 40, 50 and 60 °C), resulting in an increase in the slope of the solubility curve. This increase in the slope of the solubility curve may be related to the liberation of water molecules bound in the cavity of CDs on elevation of temperature [21]. The decrease in K_C values with increasing temperatures indicates the exothermic nature of inclusion complexation. Typical van't Hoff plots confirmed fairly well to linear behavior over the temperature range of 25–60 °C (Figure 4). Thermodynamic parameters were determined from the dependence of the K_C values on temperature in water medium (Table 1).

Characterization of complexes

Differential Scanning Calorimetry (DSC): The existence of an interaction between two components can be obtained by thermal analysis (DSC). When guest molecules are included in the CD cavity, their melting, boiling and sublimation points usually shift to a different temperature or disappear [22]. DSC thermograms of pure VAL, BCD, PM and FD complex are shown in Figure 5. A DSC thermogram of VAL exhibited a sharp endothermic peak at 173.1 °C, corresponding to its melting point (172–174 °C). The DSC thermogram of BCD showed a broad endotherm in the range of 65 °C to 110 °C, which can be attributed to desolvation of water molecules

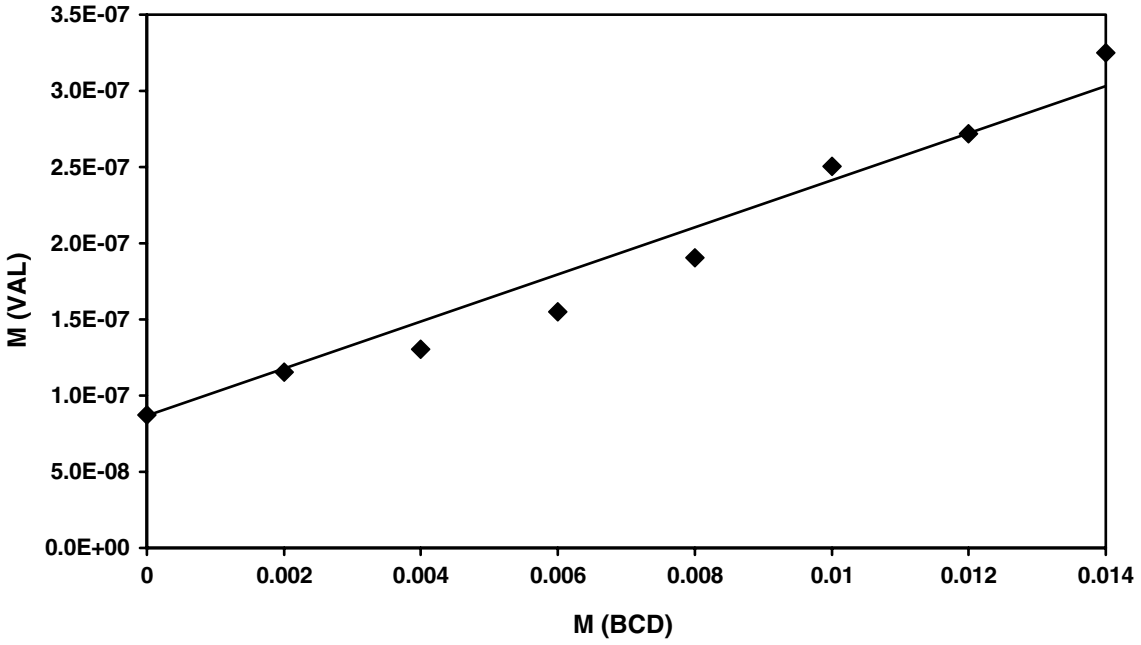

Figure 3. Phase solubility diagram of valdecoxib-β-cyclodextrin system at 25 °C.

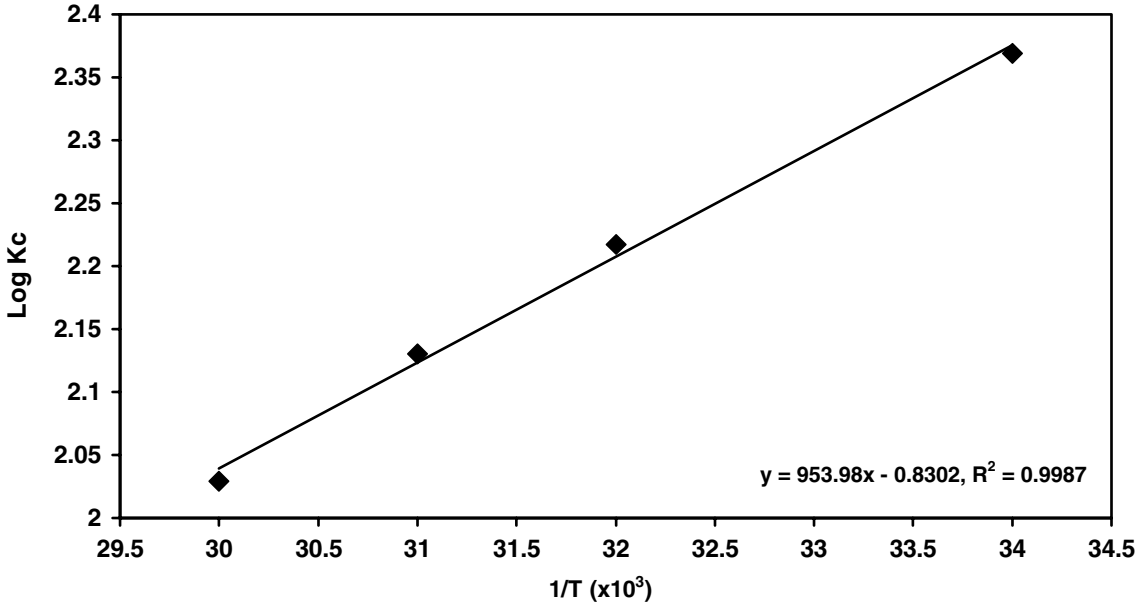

Figure 4. van't Hoff Plot of valdecoxib-β-cyclodextrin system at 25, 40, 50 and 60 °C.

present in BCD cavity. The endothermic peak of VAL was retained at 173.1 °C along with a broad endotherm in the range of 65–110 °C in PM. This may be attributed to presence of less or no interaction between the pure components in the PM. The endothermic peak of VAL was absent in FD complex.

Powder X-ray Diffractometry (P-XRD): Powder XRD is used to measure the crystallanity of the formed complex. The peak position (angle of diffraction) is an indication of a crystal structure, and peak heights are the measure of sample crystallanity in a diffractogram [23]. The formation of a diffuse diffraction pattern, appearance of new peaks, and disappearance of characteristic peaks of the guest are reported as evidence for formation of inclusion complex of drug with CD [24, 25]. Crystallanity was determined by comparing some representative peak heights in the diffraction pattern of FD with those of a reference (VAL). The relationship used for the calculation of crystallanity was relative degree of crystallanity (RDC) = I_{sam}/I_{ref}, where I_{sam} = the peak height of the sample under investigation and I_{ref} = the peak height at the same angle for the reference [26].

The P-XRD patterns and data of pure VAL, BCD, PM and FD are represented in Figure 6 and Table 2. The diffractogram of BCD exhibited characteristic peaks at 9.49, 10.83, 12.77, 13.42, 14.45, 16.63, 18.08, 18.19, 18.72, 19.04, 22.04 and 23.95 due to its crystalline nature. VAL exhibited a series of intense peaks at 12.23, 15.44, 15.81, 16.69, 17.08, 18.17, 19.81, 20.58, 22.01, 22.52, 23.84, 25.18, 27.29, 28.53 and 31.2, which were indicative of crystalline nature of VAL. Most of the principal peaks of VAL and BCD were present in the diffraction patterns of PM. This indicated that there was no interaction between the pure components of PM. In contrast to these observations, FD showed disappearance of characteristic peaks of VAL at 15.44, 19.81 and 22.01 while the RDC value were 0.2281 (at 12.23), 0.3688 (at 15.81), 0.0661 (at 23.84), 0.0953 (at 28.53). Moreover, the diffraction pattern of the peaks of FD was more diffused as compared to pure components (VAL and BCD). These observations were indicative of the transformation of VAL from crystalline to amorphous state which might be because of inclusion of VAL into BCD cavity.

Table 1. Thermodynamic parameters for the complexation of VAL with BCD

Temperature (°C)	K_c	$\Delta G°$ (Kcal/mol)	$\Delta H°$ (Kcal/mol)	$\Delta S°$ (cal/deg.mol)
25	234	−3.2325	−4.3677	−3.8093
40	165	−3.1778		−3.8015
50	135	−3.1503		−3.7690
60	107	−3.0940		−3.8249

Fourier transform infrared (FTIR) Spectroscopy: Supporting evidence for complexation of a guest molecule with the BCD can be obtained by IR spectroscopy. Although IR spectroscopy can be utilized as a supporting evidence for inclusion complex formation, many authors have reported the limited use of this technique in identifying complexation of CDs [27, 28]. FTIR spectrum of VAL (Figure 7) showed characteristic absorption bands at 1158.7 and 1347.1 cm^{-1} which may be attributed to the S = O symmetric and asymmetric stretching respectively. It also showed absorption bands at 1556 cm^{-1} (NH bend), 792 cm^{-1} (aromatic CH bend) and 1617.4 cm^{-1} (C=N stretch). FTIR spectrum of BCD showed a broad absorption band at 3394 cm^{-1} due to –OH stretching. BCD also showed absorption bands at 2935.0 cm^{-1} (C—H aliphatic stretch) and 1036.5 cm^{-1} (O—H primary sugar stretch). FTIR spectrum of FD showed very negligible changes in the absorption

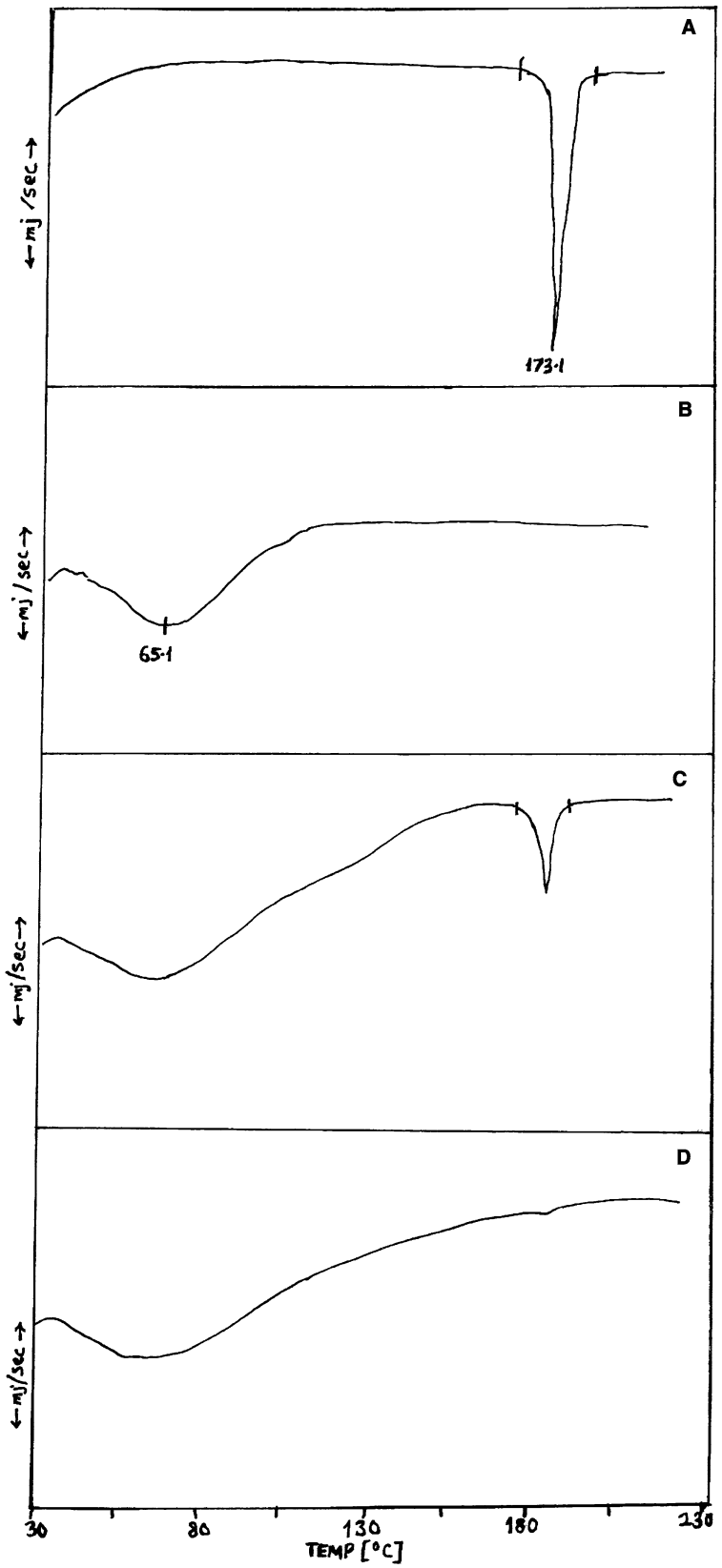

Figure 5. DSC thermograms of (a) VAL, (b) BCD, (c) PM and (d) FD complex.

frequencies of characteristic bands of VAL and BCD as compared to pure components. However, small changes in the IR wave number value (Table 3) of phenyl sulfonamide and isooxazole ring indicated that these parts of VAL are not entering into the hydrophobic cavity of BCD.

^{1}H-NMR Spectroscopy: In NMR analysis, formation of inclusion complexes of CDs is normally

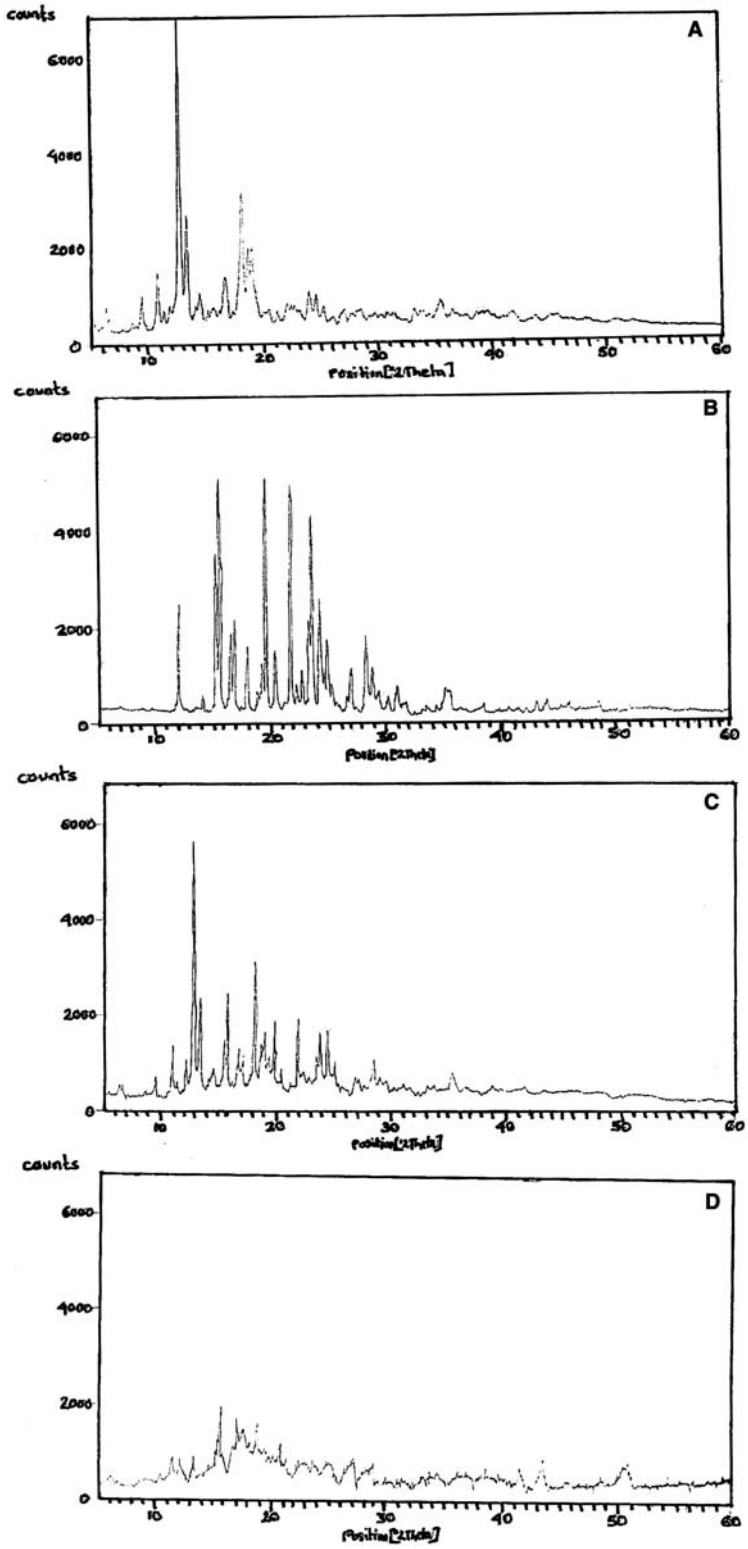

Figure 6. P-XRD diffractograms of (a) BCD, (b) VAL, (c) PM and (d) FD complex.

evidenced by changes in chemical shifts of both the host and guest molecules [29]. These chemical shift changes may provide an insight into the inclusion mode of the complex. In the present study, owing to the extremely poor aqueous solubility of VAL, water could not be used; instead DMSO solvent was used for solubilizing VAL. ^{1}H-NMR signals of VAL and BCD were assigned according to NMR information given in the references [30, 31] respectively. The chemical shift values of BCD in presence and absence of VAL (1:1 M) are summarized in Table 4 as the complexed state (δ_c), free CD state (δ_0) and chemical shift change

Table 2. P-XRD data of VAL, BCD, PM and FD complex

VAL		BCD		PM		FD	
°2θ	Height (cts)	°2θ	Height (cts)	°2θ	Height (cts)	°2θ	Height (cts)
12.23	2141.52	9.49	682.39	9.44	520.32	12.36	488.59
15.44	3257.16	10.83	1178.69	10.90	992.78	15.77	1632.14
15.81	4424.89	12.77	6518.20	12.77	5322.72	16.70	824.86
16.69	1536.74	13.42	2340.63	13.38	1948.82	17.16	1360.35
17.08	1716.48	14.45	765.77	15.40	1271.47	18.99	1030.25
18.17	1320.91	16.63	1116.87	15.76	2000.87	20.80	511.10
19.81	4631.30	18.08	2677.30	16.64	1055.83	22.54	226.59
20.58	1194.32	18.19	2764.59	18.13	2913.72	23.92	247.48
22.01	4071.43	18.72	1691.51	18.64	1115.40	25.03	207.12
22.52	580.90	19.04	1742.90	18.95	1344.70	27.25	218.68
23.84	3743.00	22.04	514.05	19.75	1604.68	28.27	144.81
25.18	1414.24	23.95	735.80	21.96	1614.95	31.70	61.46
27.29	882.11	–	–	23.50	823.25	–	–
28.53	1518.11	–	–	23.79	1305.14	–	–
31.23	587.66	–	–	24.47	1329.36	–	–

$\Delta\delta$ (ppm) ($\Delta\delta = (\delta_c - \delta_0)$). It is known that the H3′and H5′ protons of CDs located inside the cavity (Figure 8) are subjected to the up field shift owing to the ring current effect and/or the hydrophobic effect of included guest molecules [32]. Moreover, it is has been inferred that if only H3′ proton undergoes a shift in the presence of the guest molecule then the cavity penetration is shallow, whereas if H5′also shifts, then the penetration is deep [33].

The observable changes in the chemical shift upon complexation are relatively modest in the magnitude. In this study, comparatively a significant negative (up filed) chemical shift was observed for H3′ proton of BCD while other protons including H5′ were not appreciably shifted. The chemical shift values of VAL in presence and absence of BCD are summarized in Table 5. The protons of unsubstituted phenyl ring are shifted up field in more magnitude as compared to other protons of VAL. These observations reveled that penetration of VAL into BCD cavity is not deep but rather shallow and unsubstituted phenyl ring of VAL showed favorable interactions with hydrophobic cavity of BCD.

Molecular modeling studies

The final energy minimized VAL-BCD complex is shown in Figure 9. The unsubstituted phenyl ring of VAL is buried into the BCD cavity formed by 2′-hydroxyls (secondary face). The phenyl sulfonamide and polar atoms of isooxazole are exposed to the solvent. The intermolecular interaction energies are shown in Table 6. The major contribution to the stabilization of the complex is dispersive (attractive) van der Waals interaction energy. There are no hydrogen bonds between VAL and BCD observed. Table 7 summarizes changes in the solvent-accessible polar and hydrophobic surface area, as calculated from Jurs descriptors, of VAL upon complexation with BCD. There is no significant change in the total polar surface area, but the total hydrophobic surface area of VAL decreases by 32% upon complexation with BCD. Since VAL is conformationally restricted molecule, there are little changes in the phenyl ring torsion angles upon complexation with BCD (Table 8).

In vitro *dissolution studies*

The dissolution profiles of VAL, PM, KM, SM and FD are illustrated in Figure 10. The reported values are arithmetic mean of three measurements. The dissolution profile of all components exhibited first order release rate kinetics and the results are expressed as $t_{25\%}$, $t_{50\%}$, $t_{75\%}$ and $t_{90\%}$ (Table 9). The results in terms of dissolution efficiency (DE), percent of active ingredient dissolved (DP) and relative dissolution rate (RDR) are collected in Table 10. One-way analysis of variance (ANOVA) showed a significant ($p < 0.05$) increase in the dissolution rates in FD as compared to PM and pure VAL. The dissolution rate expressed by $t_{50\%}$ of FD ($t_{50\%} < 5$ min) was much faster than VAL alone ($t_{50\%} = 149.77$ min), while PM showed value of $t_{50\%} = 38.75$ min.

At 20 min the mean percent release of the drug increased 4.33 fold from FD as compared to VAL alone. PM also showed 2.24-fold increase in mean percent drug release as compared to pure drug. It was evident from the dissolution data (Table 10) that more than 85% of the drug is released in 20 min from FD while drug alone required 60 min to dissolve mere 21% of drug. This type of release data (FD) is likely to result in faster onset of action. It is also evident that the FD, SM and KM exhibited higher dissolution rates than PM and pure VAL. The extent of the enhancement of dissolution rate was found to be dependant on the preparation method of complex.

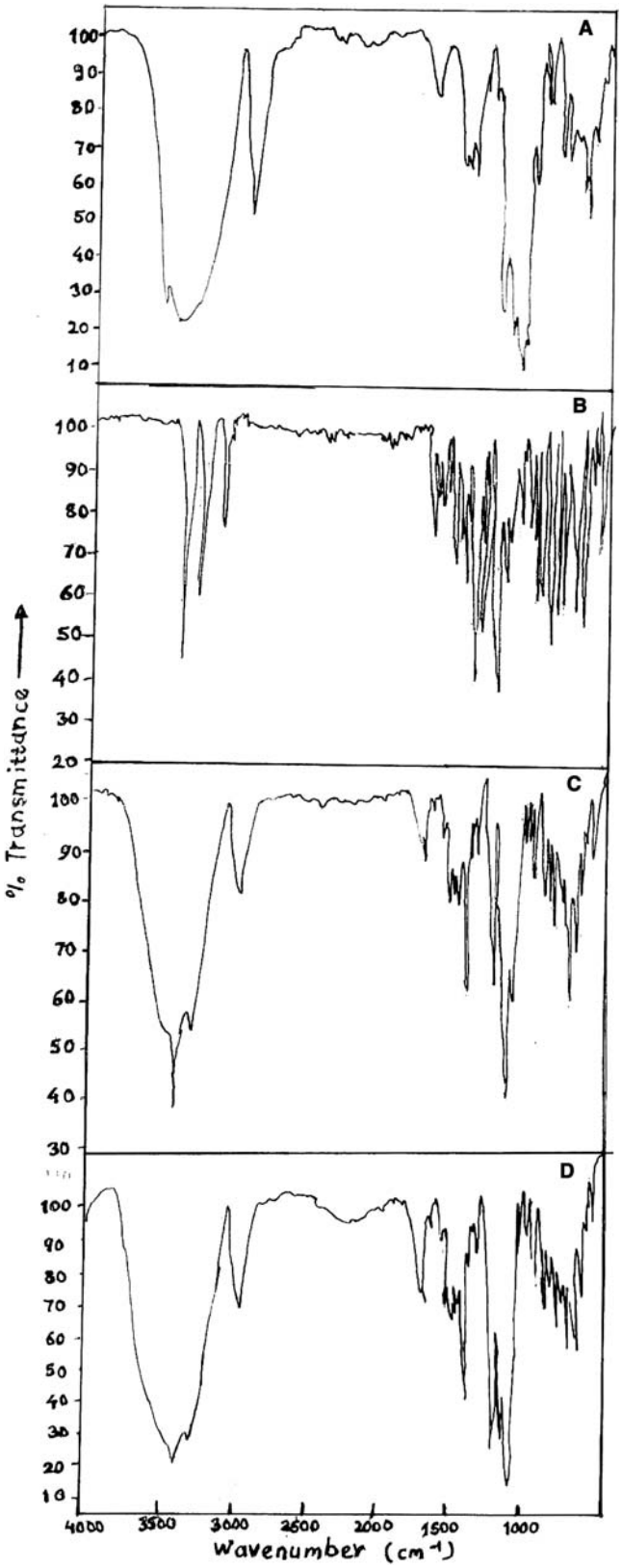

Figure 7. FTIR spectrums of (a) BCD, (b) VAL, (c) PM and (d) FD complex.

Dissolution of freeze dried VAL was also carried out and showed a slightly lower dissolution compared to pure VAL at later stage, although FD showed fastest dissolution amongst all systems.

Table 3. Changes of IR absorption frequencies of VAL and BCD in FD complex

Group Assignment	Wave Number (cm^{-1})		Δ cm^{-1}
	VAL	VAL in complex	
S=O stretch	1158.7	1153.6	−5.1
	1347.1	1342.0	
C=N stretch	1617.4	1617.0	−0.4
	BCD	BCD in complex	
C=H (aliphatic stretch)	2935.0	2935.8	+0.8
O=H (primary sugar stretch)	1036.5	1041.6	+5.1

Table 4. VAL induced ^1H chemical shift changes of BCD protons

Proton	Chemical Shift (ppm)		
	δ_C	δ_O	$\Delta\delta$
H1′	4.823	4.825	−0.002
H2′	3.297	3.298	−0.001
H3′	3.588	3.656	−0.068
H4′	3.346	3.349	−0.003
H5′	3.553	3.558	−0.005
H6′	3.626	3.628	−0.002

Discussion

Phase solubility analysis indicated the formation of first-order soluble complexes. The stability constant obtained (234.01 M^{-1}) was within the range of 100–5000 M^{-1}, which is considered as adequate for the formation of stable inclusion complex, which may contribute to the improvement of bioavailability of poorly water soluble drugs [2, 34].

Thermodynamic parameters (Table 1) showed that the inclusion complex phenomenon is predominantly due to favorable enthalpy changes which could still compensate more for the unfavorable entropy changes. In other words, negative ΔH value suggested that inclusion of VAL into BCD is an enthalpy driven process. While negative value of ΔS suggested that more water molecules are bound to the products than reactants [35]. This indicated that hydrophobic interactions are not the predominant factor for complex formation but rather other intermolecular forces such as dipole–dipole interactions might be responsible.

DSC studies showed the absence of an endothermic peak of VAL at 173.1 °C in FD, which suggested the absence of a free drug. This may also be attributed to the formation of an amorphous solid product, encapsulation of the drug inside the BCD cavity, or both [36, 37].

P-XRD analysis showed that the FD complex has a completely different pattern compared to the pure raw materials. It was no longer possible to distinguish some of the characteristic peaks of VAL, thus confirming the existence of new amorphous form in FD.

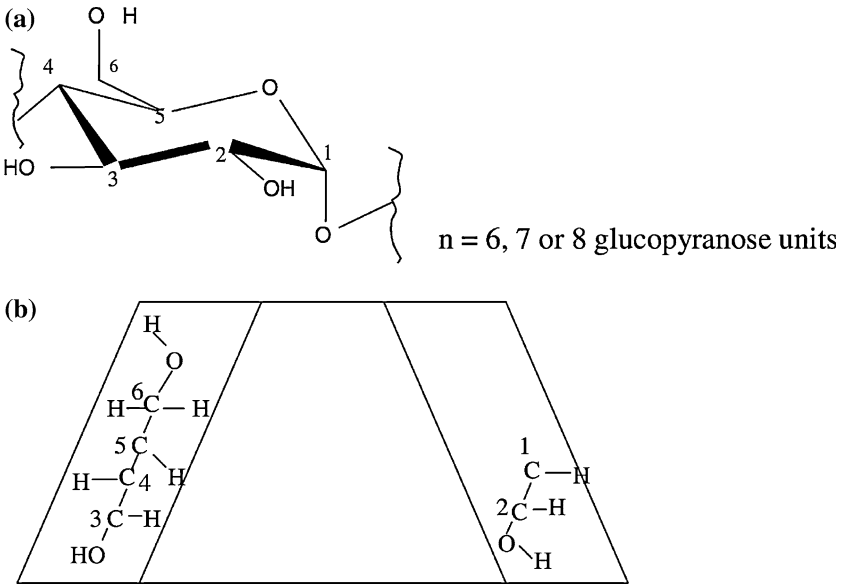

Figure 8. (a) Glucopyranose unit of CD molecule. The primary hydroxyls at 6-position exist on the primary face and secondary hydroxyls at 2- and 3-positions exist on the secondary face. (b) Schematic representation of a CD cross-section.

Table 5. BCD induced ^{1}H chemical shift changes of VAL protons

Proton	Chemical Shift (ppm)		
	δ_C	δ_O	$\Delta\delta$
a	7.836	7.842	−0.006
b	7.406	7.410	−0.004
c	7.353	7.365	−0.012
d	2.500	2.501	−0.001
e	7.333	7.339	−0.006
f	7.438	7.448	−0.010

NMR is the major technique used to prove the formation of inclusion complexes involving CDs [38]. ^{1}H-NMR analysis showed an appreciable shift for H3′ protons along with no major shifts for H5′ protons indicated shallow penetration of BCD through secondary face. Chemical shifts observed with protons of VAL suggested the possible interaction of unsubstituted phenyl ring of VAL with H3'proton of BCD. However, it should be noted that the added DMSO might reduce the binding strength of VAL–BCD complex (possibly via binding competition or VAL extraction) but will not significantly alter the basic mode of interaction [39, 40].

Modeled complex revealed that dispersive (attractive) van der Waals interaction energy is major contributor for stabilization of complex which is complementary with the thermodynamic data which indicated role of non-bonded interactions in the process of complex formation. The energy-minimized complex showed that the hydrogen bond interactions are not present in complex which is also revealed from the thermodynamic parameters. ^{1}H-NMR and molecular modeling study revealed that unsubstituted phenyl ring is shallowly buried in the BCD cavity while isooxazole ring and phenyl sulfonamide do not insert in the cavity which was also revealed in FTIR data showing phenyl sulfonamide and isoxazole are not having any interaction with BCD cavity. Significant decrease in the total hydrophobic surface area (32%) of VAL upon complexation with BCD might be responsible for increased solubility of VAL in the inclusion complex state. The data of modeled drug corroborate well with the experimental data suggesting that the molecular modeling can be used as a complementary tool for characterizing the inclusion complexes of drug with CDs.

The improved dissolution of FD may be due to the formation of an inclusion complex of the drug with BCD and/or the conversion of drug to an amorphous state. Dissolution of freeze dried VAL showed a slight lower dissolution compared to pure VAL at later stage, which may be attributed to agglomerate formation and/or recrystallization. Dissolution studies showed the PM also showed better dissolution rate compared to VAL alone. This may be explained on the basis of the solubility of VAL in aqueous BCD solution. Since BCD dissolve more rapidly in the dissolution medium than the pure drug, it can be assumed that, in early stages of the dissolution process (evident from DP of PM up to 20 min, Figure 10), the BCD molecules will operate locally on the hydrodynamic layer surrounding the particles of drug. This action results in an *in situ* inclusion process, which produces a rapid increase of the amount of the dissolved drug [29].

The extent of the enhancement of dissolution rate was found to be dependant on the preparation method of complex. The dissolution rate improvement in case of PM and KM may be due to only wetting effect of BCD; in fact this effect is more pronounced in case of KM where the mixing process between the two component is more intensive which may result into formation of metastable state of drug. The SM showed slightly lower

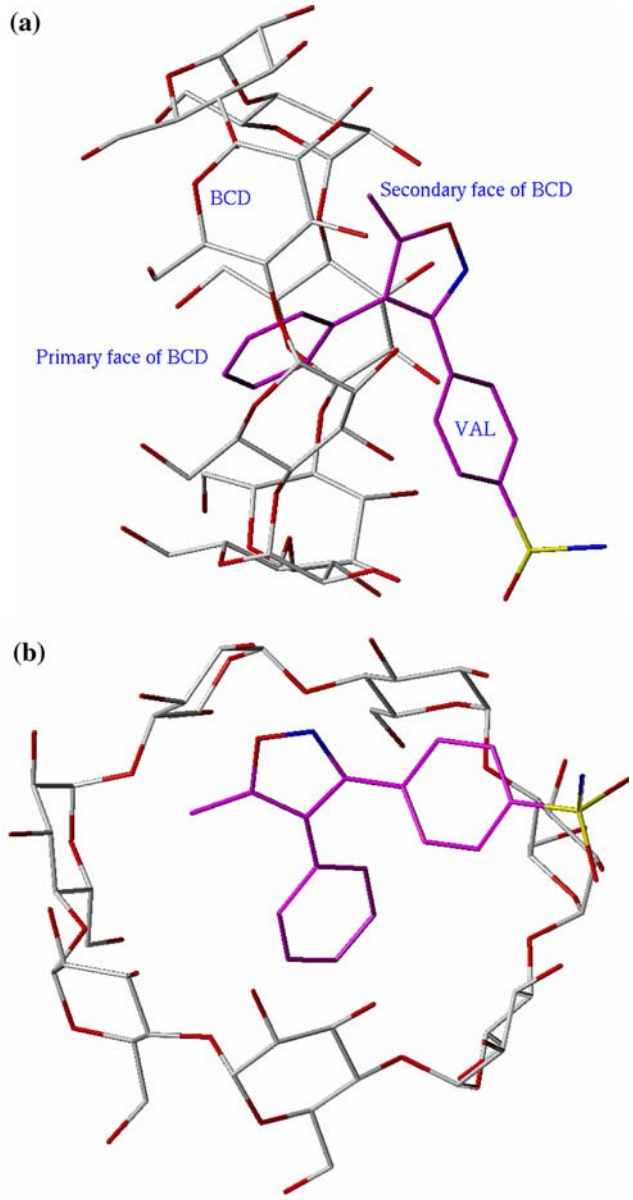

Figure 9. Orientation of valdecoxib molecule in β-cyclodextrin cavity after molecular dynamic simulations: (a) side view (b) top view.

dissolution as compared to FD, which may be due to inefficient complexation of drug with BCD. This may happen because of precipitation of drug during complexation process itself leaving free drug in the complexation medium.

The dissolution rates from CD complexes of drug is influenced by enhanced particle wettability and decreased crystallanity by inclusion complexation [41], diffusion and dissociation of complex in the dissolution medium, and surfactant-like effect of CDs [42].

In the present investigation, the improvement in dissolution rate is attributed to the increased solubility and wettability due to encapsulation along with decreased crystallanity caused by inclusion complexation, which was evident from DSC and P-XRD studies. These results are in agreement with the molecular modeling data (which showed significant reduction in total hydrophobic surface area of VAL upon complexation with BCD) and phase solubility analysis.

Table 7. Changes in solvent-accessible polar and hydrophobic surface area of VAL upon complexation with BCD

Molecule	TPSA	THSA	% decrease in THSA
BCD	760.8	460.9	32
VAL	163.5	377.5	
VAL-BCD	685.8	533.8	

TPSA: Total polar surface area; THSA: Total hydrophobic surface area.

Table 8. Changes in torsion angles of VAL upon complexation with BCD

	BC	AC	Difference
Isooxazole with phenyl sulfonamide	161	168	+7
Sulfonamide with phenyl ring	90	59	−31
Isooxazole with phenyl ring	146	153	+7

BC: Before Complexation; AC: After Complexation.

Conclusion

The present study clearly demonstrated that the aqueous solubility of valdecoxib can be substantially increased via complexation with BCD. The data obtained from DSC, P-XRD, FTIR and NMR studies showed that it is possible to obtain a true inclusion complex of valdecoxib with BCD by freeze–drying method. The results from MD simulations are in good accord with the experimental data. The increased solubility and dissolution rates obtained with VAL–BCD inclusion complex can have greater utility in the fast-dissolving dosage

Table 6. Intermolecular interaction energies of VAL, BCD and VAL-BCD complex

Molecule	Internal Energy	VdW Repulsion	VdW Dispersion	Electrostatic	Total Non bond Energy	Total Energy
BCD	63.3	255.0	−203.8	99.9	151.1	214.4
VAL	82.0	128.1	−59.8	−28.4	39.9	121.9
BC	145.4	383.0	−263.6	71.5	191.0	336.3
AC	136.8	406.8	−322.3	79.6	164.1	301.0
AC-BC	−8.6	23.8	−58.7	−8.0	−26.8	−35.4

BC: Before Complexation; AC: After Complexation.

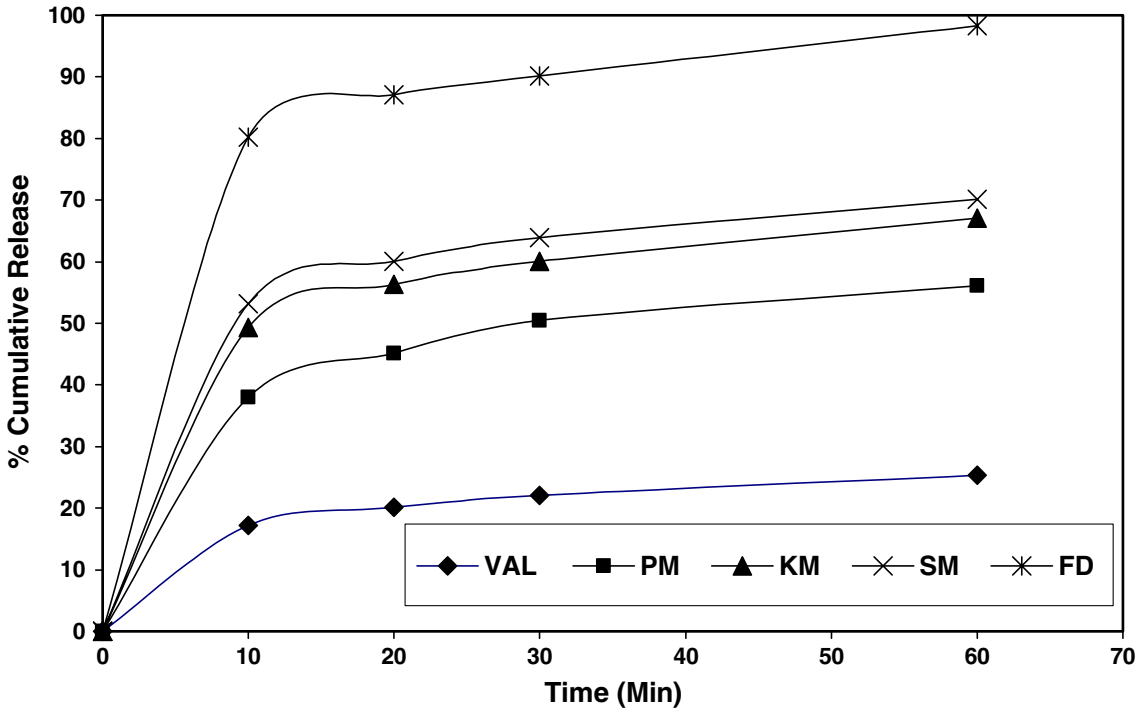

Figure 10. Dissolution profiles of VAL, PM, KM, SM and FD in water ($n = 3$).

Table 9. Dissolution rate data of VAL, PM, KM, SM and FD

System	$t_{25\%}$(min)	$t_{50\%}$(min)	$t_{75\%}$(min)	$t_{90\%}$(min)
VAL	48.28	149.77	323.26	552.58
PM	4.06	38.75	98.04	176.42
KM	< 1	23.03	67.94	127.30
SM	< 1	18.74	60.34	115.33
FD	< 1	2.48	13.76	28.68

forms with the possible enhancement of oral bioavailability and faster onset of action.

Acknowledgements

The authors are grateful to Unichem Laboratories Ltd., India and Cerestar Inc., USA for providing gift samples of valdecoxib and β-cyclodextrin respectively. The authors are also thankful to Dr. Sudha Srivastava of TIFR, Mumbai for providing NMR facility. The authors are also thankful to the University Grants Commission (UGC), India for providing financial support.

References

1. S.H. Yalkowsky: Techniques of Solubilization of Drugs, Marcel and Dekker (1981), p.15.
2. J. Blanco *et al.*: *Drug. Dev. Ind. Pharm.* **17**, 943 (1991).
3. M.G. Fucile *et al.*: *Eur. J. Pharm. Biopharm* **38**, 140 (1992).
4. T. Loftsson and E.M. Brewster: *J. Pharm. Sci.* **85**, 1017 (1996).
5. G. Moster and D. Thompson: Encyclopedia of Pharmaceutical Technology, vol 19, Marcel Dekker, Inc., New York, p. 49.
6. J.J. Talley *et al.*: *J. Med. Chem.* **43**, 775 (2000).
7. M.L. Chavez and C.J. Dekorte: *Clin. Ther.* **25**, 817 (2002).
8. R.W. Mc Murr and K.J. Hardy: *Amer. J. Med. S.* **323**, 181 (2002).
9. N.A. Kasim *et al.*: *Molecular Pharmaceutics* **1**(1), 85 (2004).
10. P.C. Isakson *et al.*: *Gastroenterol. Internat.* **12**, 169 (1999).
11. T. Loftsson: *Pharm. Technol. Eur.* **11**, 20 (1999).
12. K.B. Lipkowitz: *Chem. Rev.* **98**, 1829 (1998).
13. J.M. Madrid *et al.*: *J. Phys. Chem. B.* **103**, 4847 (1998).
14. F. Melani *et al.*: *Int. J. Pharm.* **166**, 145 (1998).
15. F.J. Oteri-Espinar *et al.*: *Int. J. Pharm.* **7**, 149 (1992).
16. T. Higuchi and K.A. Connors: *Adv. Anal. Chem. Instr.* **4**, 117 (1965).
17. M. Adachi *et al.*: *J. Biol. Chem.* **273**(31), 19859 (1998).
18. K.A. Khan: *J. Pharm. Pharmacol.* **27**, 48 (1975).
19. K. Uekama *et al.*: *Chem. Rev.* **98**, 2045 (1998).
20. K. Uekama *et al.*: *Applications of Cyclodextrins*, Harwood Academic Publishers, London (1977), pp. 411.
21. K. Shinoda and Fujihira: *Bull. Chem. Soc. Jap.* **41**, 2612 (1968).
22. H. Cabralmarques *et al.*: *Int. J. Pharm.* **63**, 259 (1990).
23. M.D. Veiga *et al.*: *J. Pharm. Sci.* **87**, 891 (1998).

Table 10. Dissolution profile data of VAL, PM, KM, SM and FD

System	$DE(\%)_{20\ min}$	$DP_{20\ min}$	$RDR_{20\ min}$	$DE(\%)_{60\ min}$	$DP_{60\ min}$	$RDR_{60\ min}$
VAL	13.62 ± 0.8	20.13 ± 0.9	–	19.89 ± 0.9	25.33 ± 0.7	–
PM	30.28 ± 0.9	45.13 ± 1.0	2.24	44.70 ± 1.1	56.12 ± 0.9	2.22
KM	38.77 ± 0.7	56.32 ± 0.8	2.80	54.44 ± 0.7	67.12 ± 0.8	2.65
SM	41.60 ± 0.4	60.12 ± 0.6	2.99	57.71 ± 0.4	70.13 ± 0.6	2.77
FD	61.88 ± 0.2	87.13 ± 0.5	4.33	82.52 ± 0.3	98.32 ± 0.5	3.88

DE : Dissolution efficiency, DP : Percentage of dissolved drug , RDR : Relative dissolution rate (with reference to pure drug).

24. M.D. Veiga and F. Ahsan: *Chem. Pharm. Bull.* **48**, 793 (2000).
25. C.M. Fernandes *et al.*: *Eur. J. Pharm. Sci.* **15**, 79 (2002).
26. J.A. Ryan *et al.*: *J. Pharm. Sci.* **75**, 805 (1986).
27. G. Becket *et al.*: *Int. J. Pharm.* **179**, 65 (1999).
28. O.I. Corrigan and C.T. Stanley: *J. Pharm. Pharmacol.* **34**, 621 (1982).
29. F. Djedaini *et al.*: *Pharm. Res.* **79**, 643 (1990).
30. J.J. Yuan *et al.*: *Drug Met. Dispo.* **30**(9), 1013 (2002).
31. H. Schneider *et al.*: *Chem. Rev.* **98**, 1755 (1998).
32. M.L. Bender and M. Komiyama: *Cyclodextrin Chem*, Springer-Verlag, Berlin (1978).
33. K.A. Connors: *Chem. Rev.* **97**, 1325 (1997).
34. T. Yamada *et al.*: *Chem. Pharm. Bull.* **48**, 1264 (2000).
35. K. Uekeama *et al.*: *Chem. Pharm. Bull.* **26**, 1162 (1978).
36. M.T. Escusa- Diaz *et al.*: *Eur. J. Pharm. Sci.* **4**, 291 (1994).
37. P. Mura *et al.*: *Drug. Dev. Ind. Pharm.* **25**, 279 (1999).
38. A.R. Hedges: *Chem. Rev.* **98**, 2035 (1998).
39. T. Matsui *et al.*: *Biosci. Biotech. Biochem.* **58**, 1102 (1994).
40. E. Junquera *et al.*: *J. Colloid. Interface. Sci.* **216**, 154 (1999).
41. R.B. Gandhi *et al.*: *Drug. Dev. Ind. Pharm.* **14**, 657 (1988).
42. M. Donbrow *et al.*: *J. Pharm. Sci.* **67**, 95 (1978).